Journal of Cellular and Molecular Medicine
A JOURNAL OF TRANSLATIONAL MEDICINE

J. Cell. Mol. Med. Vol 15, No 11, 2011 pp. 2512-2524

Identification of protein targets underlying dietary nitrate-induced protection against doxorubicin cardiotoxicity

Lei Xi *, Shu-Guang Zhu, Daniel C. Hobbs, Rakesh C. Kukreja

VCU Pauley Heart Center, Division of Cardiology, Department of Internal Medicine, Virginia Commonwealth University, Richmond, VA, USA

Received: September 20, 2010; Accepted: January 4, 2011

Abstract

We recently demonstrated protective effect of chronic oral nitrate supplementation against cardiomyopathy caused by doxorubicin (DOX), a highly effective anticancer drug. The present study was designed to identify novel protein targets related to nitrate-induced cardioprotection. Adult male CF-1 mice received cardioprotective regimen of nitrate (1 g $NaNO_3$ per litre of drinking water) for 7 days before DOX injection (15 mg/kg, i.p.) and continued for 5 days after DOX treatment. Subsequently the heart samples were collected for proteomic analysis with two-dimensional differential in-gel electrophoresis with 3 CyDye labelling. Using 1.5 cut-off ratio, we identified 36 proteins that were up-regulated by DOX in which 32 were completely reversed by nitrate supplementation (89%). Among 19 proteins down-regulated by DOX, 9 were fully normalized by nitrate (47%). The protein spots were further identified with Matrix Assisted Laser Desorption/Ionization-Time-of-Flight (MALDI-TOF)/TOF tandem mass spectrometry. Three mitochondrial antioxidant enzymes were altered by DOX, *i.e.* up-regulation of manganese superoxide dismutase and peroxiredoxin 3 (Prx3), and down-regulation of Prx5, which were reversed by nitrate. These results were further confirmed by Western blots. Nitrate supplementation also significantly improved animal survival rate from 80% in *DOX* alone group to 93% in *Nitrate + DOX* group 5 days after the DOX treatment. In conclusion, the proteomic analysis has identified novel protein targets underlying nitrate-induced cardioprotection. Up-regulation of Prx5 by nitrate may explain the observed enhancement of cardiac antioxidant defence by nitrate supplementation.

Keywords: nitrate • cardioprotection • doxorubicin • cardiotoxicity • proteomics • 2D-DIGE • antioxidant

Introduction

Doxorubicin (DOX) is a highly effective anthracycline anticancer drug that has been used for more than four decades to treat a variety of human neoplasms [1]. The well-recognized cardiotoxic side effect of DOX, which may lead to irreversible dilated cardiomyopathy and heart failure [2, 3] has been a dilemma for both oncologists and cardiologists around the world and seriously limited its use in the treatment of many cancer patients. Despite intensive research in the past decades, an optimal therapeutic intervention for protecting heart against DOX-induced cytotoxicity has not been identified. Dexrazoxane is the only compound currently approved by U.S. Food and Drug Administration in September 2007 for protection against anthracycline-induced tissue injuries such as extravasation. However, due to the cytotoxic side effect and limited efficacy of dexrazoxane, there is an ongoing need for a better drug for protecting heart against DOX-induced cardiotoxicity [4].

The cardioprotective role of nitric oxide has been demonstrated in numerous animal models of myocardial damage such as ischemia-reperfusion injury [5–8]. The nitrate/nitrite/nitric oxide pathway is a crucial complementary or alternative system to the nitric oxide synthase dependent pathway for ensuring sufficient nitric oxide production, especially under pathophysiological conditions such as hypoxia and acidosis when the oxygen-dependent NOS activities are compromised [9, 10]. As a substantial portion of nitrate/nitrite in the body is derived from dietary sources, dietary supplementation of nitrate or nitrite was shown to attenuate myocardial ischemia-reperfusion injury [11, 12] and hypertension [13, 14]. We recently showed the protective effects of chronic oral nitrate intake against DOX-induced cardiac contractile dysfunction, myocyte necrosis/apoptosis and mitochondrial respiratory chain damages [15, 16]. To further explore the molecular mechanisms underlying nitrate-induced protection against DOX cardiotoxicity,

*Correspondence to: Lei XI, M.D.,
Division of Cardiology, Box 980204,
Virginia Commonwealth University,
1101 East Marshall Street, Room 7–020C,
Richmond, VA 23298–0204, USA.
Tel.: (804)-628–5533
Fax: (804)-828–8700
E-mail: lxi@vcu.edu

doi: 10.1111/j.1582-4934.2011.01257.x

we designed this study to identify novel protein targets that are altered by treatment with DOX and chronic nitrate supplementation using a state-of-the-art proteomic approach with two-dimensional differential in-gel electrophoresis (2D-DIGE) and MALDI TOF/TOF tandem mass spectrometry. Our results show a number of novel protein targets that are potentially responsible for the protection of DOX-induced cardiomyopathy with nitrate supplementation.

Materials and methods

Animals

Adult male CF-1 outbred mice (body weight ~35 g) were purchased from Harlan Sprague Dawley, Inc. (Indianapolis, IN, USA). The animal experimental protocols were approved by the Institutional Animal Care and Use Committee of the Virginia Commonwealth University. All animal experiments were conducted under the guidelines on humane use and care of laboratory animals for biomedical research published by the National Institutes of Health (No. 85–23, Revised 1996).

Protocol for animal experiments

The mice were administered a single dose of DOX intraperitoneally (15 mg/kg, dissolved in saline; purchased from Sigma-Aldrich, St. Louis, MO, USA; *DOX* group) or volume-matched saline (0.2 ml; *Control* group). Another group of mice (*Nitrate + DOX* group) received chronic nitrate supplementation with $NaNO_3$ added into the drinking water at the concentration of 1 g/L (~12 mM) for 7 days before the DOX injection on day 8 and continued through the end of 5-day post-DOX period as described previously [15, 16]. Such nitrate supplementation protocol has been shown to protect against DOX-induced ventricular dysfunction [15] and mitochondrial respiratory chain damage [16]. Under surgical anaesthesia with pentobarbital sodium (70 mg/kg, i.p.), the heart samples were collected *via* thoractomy, rinsed off blood with saline and immediately frozen in liquid nitrogen and stored at –70°C until further proteomic experiments or Western blot analysis.

Two-dimensional differential in-gel electrophoresis and minimal CyDye labelling

The 2D-DIGE and mass spectrometry protein identification were performed by Applied Biomics, Inc. (Hayward, CA, USA) following established protocols. In brief, the heart tissues were washed with a buffer containing: 10 mM Tris-HCl, 5 mM magnesium acetate (pH 8.0) three times to remove the contaminated blood. For 100 mg of tissues, 2 ml of the 2D cell lysis buffer (30 mM Tris-HCl, pH 8.8, containing 7 M urea, 2 M thiourea and 4% 3-[(3-Cholamidopropyl)-dimethylammonio]-1-propane sulfonate (CHAPS) was added and subjected to sonication at 4°C. After vigorous shaking for 30 min. at room temperature, the tissue lysates were centrifuged at 4°C for 30 min. at 14,000 rpm and the supernatant was collected. Following measurement of protein concentration using Bio-Rad protein assay (Bio-Rad, Hercules, CA, USA), the lysate samples were diluted with 2D cell lysis buffer in order to obtain the equal protein concentration (5 mg/ml). Thirty micrograms of tissue lysate was labelled with 1 μl CyDye dilution (Cy2, Cy3 and Cy5, Amersham, Piscataway, NJ, USA). The CyDyes stock (1 nmol/μl) were diluted 1:5 with dimethylformamide, incubated on ice for 30 min. in dark, followed by addition of 1 μl of 10 mM lysine to stop the labelling reaction. The Cy2, Cy3 and Cy5 labelled samples were mixed with 2× 2D sample buffer [8 M urea, 4% CHAPS, 20 mg/ml dithiothreitol (DTT), 2% pharmalytes and trace amount of bromophenol blue], followed by addition of 100 μl destreak solution (GE Healthcare, Piscataway, NJ, USA) and rehydration buffer (7 M urea, 2 M thiourea, 4% CHAPS, 20 mg/ml DTT, 1% pharmalytes and trace amount of bromophenol blue) to make up the volume to 250 μl for loading into a 13 cm immobilized pH gradient (IPG) strip (pH 3–10, Linear, GE Healthcare/Amersham) and run the isoelectric focusing under dark. Upon finishing the isoelectric focusing, the IPG strips were incubated in 10 ml of equilibration buffer 1 (50 mM Tris-HCl, pH 8.8, containing 6 M urea, 30% glycerol, 2% SDS, trace amount of bromophenol blue and 10 mg/ml DTT) for 15 min., followed by incubation in 10 ml of equilibration buffer 2 (50 mM Tris-HCl, pH 8.8, containing 6 M urea, 30% glycerol, 2% SDS, trace amount of bromophenol blue and 45 mg/ml iodacetamide) for 10 min. The IPG strips were then rinsed in SDS-gel running buffer and transferred into 12% SDS-gel and sealed with 0.5% agarose solution in SDS-gel running buffer and electrophoresis was performed at 15°C.

Image scan and data analysis

Each gel was scanned immediately following SDS-PAGE using Typhoon Trio scanner (Amersham). The scanned images were then analysed by Image QuantTL software (GE Healthcare), and then subjected to in-gel analysis and cross-gel analysis using DeCyder software version 6.5 (GE Healthcare). The change in ratio of differential protein expression was obtained from in-gel DeCyder software analysis. Quantitative comparisons were then made between two individual samples for each of the three possible combinations. The pairwise volume ratios (*i.e. Control versus DOX*, *Control versus Nitrate + DOX* and *DOX versus Nitrate + DOX*) were calculated for each protein spot and used to determine relative protein expression. To simplify the data presentation, only the ratios of comparisons against *Control* are presented.

Spot picking and digestion and MALDI-TOF/TOF

The selected spots were picked up by Ettan Spot Picker (GE Healthcare) following the DeCyder software analysis and spot picking design. The selected protein spots were subjected to in-gel trypsin digestion, peptides extraction, desalting and followed by MALDI-TOF/TOF to determine the protein identity. In brief, mass spectra (MS) of the peptides in each sample were obtained using Applied Biosystems (Carlsbad, CA, USA) Proteomics Analyzer. Ten to 20 of the most abundant peptides in each sample were further subjected to fragmentation and tandem mass spectrometry (MS/MS) analysis. Protein identification was based on peptide fingerprint mass mapping (using MS spectra) and peptide fragmentation mapping (using MS/MS spectra). Combined MS and MS/MS spectra were submitted for database search using GPS Explorer software equipped with the MASCOT search engine to identify proteins from primary sequence databases.

Western blot analysis

To confirm the results of 2D-DIGE, we performed Western blots to assess expression levels of a few selected proteins. In brief, the mouse heart

samples were ground into fine powders under liquid nitrogen and homogenized with a Glas-Col® tissue homogenizer in 1 ml of ice-cold lysis buffer containing (in mM) 20 Tris*HCL pH 7.4, 150 NaCl, 1 ethylenediaminetetraacetic acid, 1 ethylene glycol tetraacetic acid (EGTA), 0.2 phenylmethylsulfonyl fluoride (PMSF), 0.2 Na_3VO_4, added with β-mercaptoethanol and a cocktail of protease and phosphotase inhibitors (Pierce, Rockford, IL, USA; product# 78440). After centrifugation at 12,000 × *g* for 15 min. (4°C), the supernatant was separated from the pellet and stored in –80°C until further analysis. Following measurement of the protein concentration with Bio-Rad protein assay kit, equal amount of protein for each sample were combined with an equal volume of a loading buffer solution made by mixing 25 μl of Laemmli sample buffer (Bio-Rad) and 475 μl β-mercaptoethanol (Bio-Rad). The samples were boiled for 5 min. before being loaded into each well on polyacrylamide gels (Bio-Rad). The gels were electrophoresed for 1 hr at 180 volts in running buffer [1× Tris/glycine/SDS]. The electrophoresed proteins were trans-blotted from the gel to nitrocellulose membranes at 400 mA for 90 min. (4°C). After placing in blocking solution containing 5% non-fat milk in 1× Tris-buffered saline and 0.05% Tween-20 (Bio-Rad) for 1 hr at room temperature, the membranes were incubated with primary antibodies overnight under 4°C at 1:1000 dilution for mitochondrial superoxide dismutase 2 (SOD2; Calbiochem, San Diego, CA, USA), myosin light chain 2 (MYL2), fatty acid binding protein 3 (FABP3), peroxiredoxin 3 (Prx3), Prx5 and brain glycogen phosphorylase (PYGB), which were supplied by Proteintech Group, Inc. (Chicago, IL, USA) and α-Tubulin (Santa Cruz Biotechnology, Santa Cruz, CA, USA). The blots were then washed and incubated with anti-rabbit (GE Healthcare) or anti-goat (Santa Cruz) secondary antibody conjugated to horseradish peroxidase at 1:2000 dilution in 5% milk in 1× TBST for 1 hr at room temperature. The membranes were then washed and the bands were visualized *via* enhanced chemiluminescence (PerkinElmer, Waltham, MA, USA) and subsequently exposed to a Kodak film. The optical density of the protein bands was quantified using Image J software. Expression for all the studied proteins was normalized to α-Tubulin expression.

Statistical analysis

The normalized densitometric results of protein expression by Western blots were analysed using one-way ANOVA followed by Student–Newman–Keuls *post hoc* test for pairwise comparison. The chi-square test was used to compare the animal survival rates between the four treatment groups. Probability value of $P < 0.05$ was considered significant.

Results

Detection of DOX-induced alterations in cardiac protein expression with 2D-DIGE

Immediately following the 2D-DIGE and SDS-PAGE procedures, the scanned images from each gel were subjected to in-gel analysis to determine the protein differential expression. Quantitative pairwise comparisons of the protein volume ratios for each protein spot were then made among the three treatment conditions (*i.e. Control versus DOX*, *Control versus Nitrate + DOX*, and *DOX versus Nitrate + DOX*). Figure 1A shows an overlay image for in-gel comparison between heart samples from control (labelled in green dye) and DOX-treated mouse (labelled in red dye). Similarly, Figure 1B depicts an overlay image for in-gel comparison between the heart samples from control (labelled in green dye) and nitrate + DOX (labelled in red dye) groups. The numbered circles represent a total of 82 protein spots that are differentiable among three treatment conditions in terms of abundance in protein expression using the 1.5 cut-off ratio. Figure 2 is a typical example of

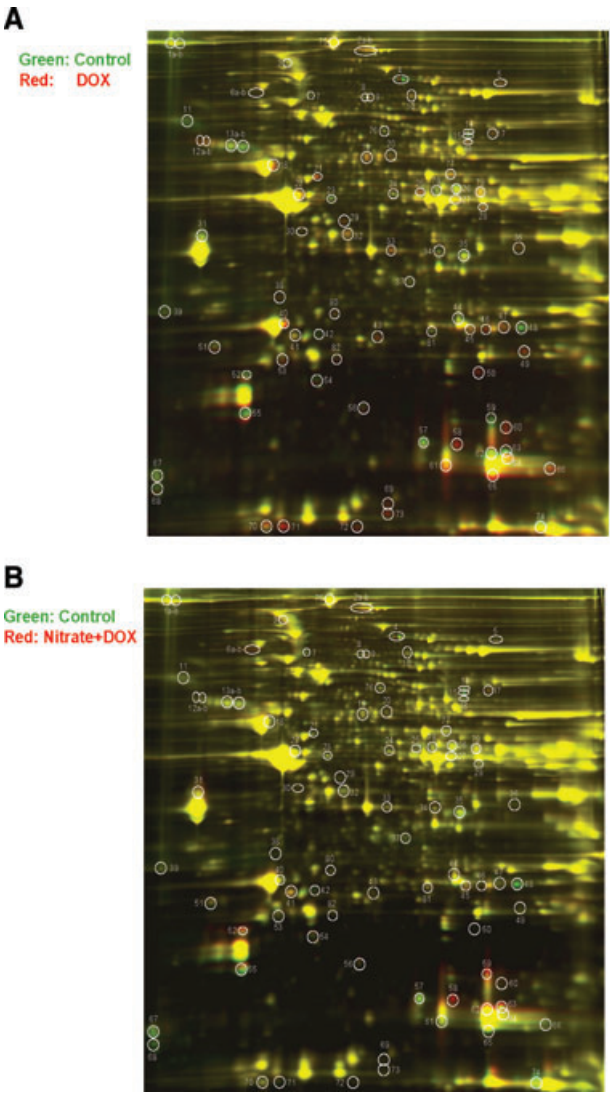

Fig. 1 Scanned images of the 2D gels. (**A**) Overlay image for in-gel comparison between hearts from *Control* (labelled in green dye) and *DOX*-treated (labelled in red dye) mice; (**B**) Overlay image for in-gel comparison between *Control* heart (labelled in green dye) and heart sample from mouse that received nitrate supplementation plus DOX injection (*Nitrate + DOX*; labelled in red dye). The circled and numbered protein spots (82 in total with a cut-off ratio of 1.5 for alteration in protein expression among the three treatment conditions) are subsequently isolated from the gels and identified by MALDI TOF/TOF mass spectroscopy.

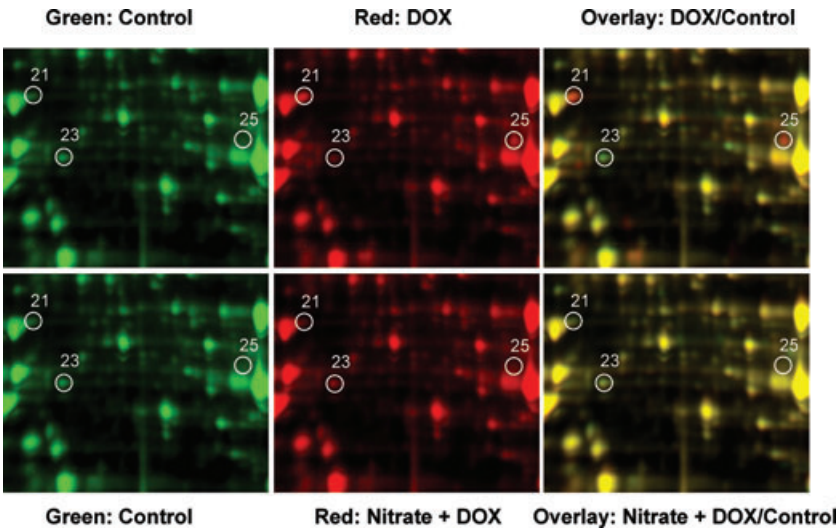

Fig. 2 Typical 2D gel images indicating DOX-induced modifications in protein expression. Top panel shows up-regulation of protein spot #21 and #25 as well as down-regulation of spot #23 in *DOX* group as compared with the *Control* group (see overlay image). Lower panel indicates the reversal of the DOX-induced changes in spots #21, #23 and #25 by nitrate supplementation (*i.e. Nitrate + DOX versus Control*).

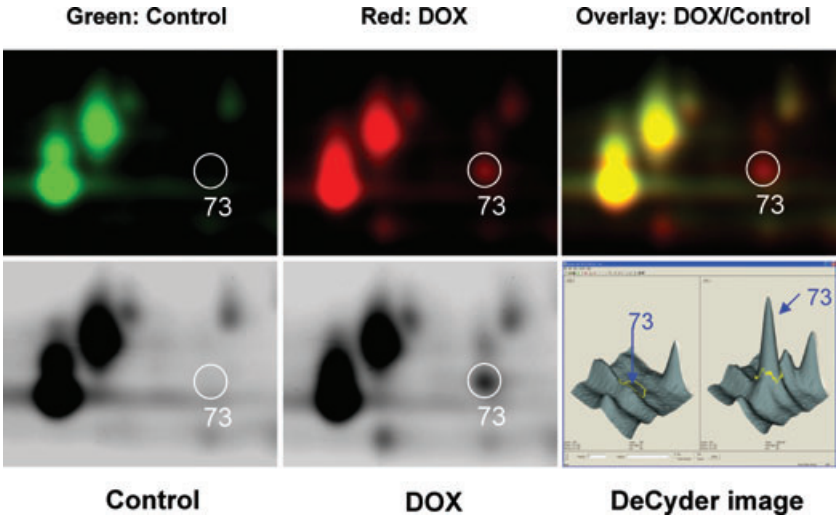

Fig. 3 Representative magnified 2D gel image focusing on an individual protein spot (#73). The differences between *Control* and *DOX* group are clearly distinguishable based on the labelled fluorescent dye colours (top panel), spot density of the converted black-and-white images (bottom panel), as well as the integrated 3D DeCyder software analysis output for this protein (bottom panel).

DOX-induced modifications in protein expression (top panel), *i.e.* up-regulation at protein spot #21 and #25 *versus* down-regulation at spot #23. It is quite obvious that DOX-induced change in colour of these spots is normalized by nitrate supplementation (see the lower panel). A representative image of individual protein spot (#73) is shown in Figure 3, which includes the distinguishable difference based on dye colours (see the top panel) and the confirmation by black-and-white gel image as well as the integrated 3D DeCyder software analysis (see the bottom panel).

From these prominently identified spots we further selected 62 protein spots that were modified (greater than ±1.5-fold) by DOX treatment for protein identification using MALDI TOF/TOF tandem mass spectrometry. We selected 41 protein spots that were up-regulated by DOX, among which three spots had no confidence on protein identification (*i.e.* #70, #71, #72) and 2 spots were matched with unnamed protein sequences (*i.e.* #56, #60). Table 1 shows results ranked from the largest to the smallest according to the fold changes of DOX/Control ratio. A total of 21 protein spots were down-regulated by DOX, in which only 1 spot had no confidence on protein identification (*i.e.* #63). Similarly, Table 2 summarizes protein spots down-regulated by DOX. Again, the rank order of the protein spots in this table is based on the DOX/control ratio fold changes, from the largest to the smallest.

Effect of nitrate supplementation on DOX-induced modification of proteins

As summarized in Table 1, among the 36 protein spots up-regulated by DOX, 32 were completely reversed by nitrate supplementation (89%), 1 was partially reversed, and only 3 were not affected (8%; *i.e.* spot #2a – *myosin binding protein C, cardiac*; spot #45 –

Table 1 Cardiac proteins up-regulated by DOX: Effects of nitrate supplementation

2D-DIGE spot no.	Top-ranked protein name	Accession no.	Protein MW (kD)	Confidence of protein ID	DOX/ control ratio	Nitrate + DOX/ control ratio	Reversed by nitrate
73	FABP3, muscle and heart	gi|6753810	14.8	High	8.04	–1.65	Yes (completely)
71	Nuclear receptor subfamily 1, group I, member 2 isoform	gi|148536879	44.9	*No* (*fragments?*)	4.82	–1.01	Yes (completely)
60	Unnamed protein product	gi|74146841	17.9	High	4.58	1.39	Yes (completely)
58	Nucleoside-diphosphate kinase 2	gi|6679078	17.4	High	4.18	5.27	No
64	Myoglobin	gi|21359820	17.1	High	3.73	–1.15	Yes (completely)
65	Myoglobin	gi|21359820	17.1	High	3.72	–1.9	Yes (completely)
50	Crystallin, $\alpha\beta$	gi|6753530	20.1	High	3.61	–1.23	Yes (completely)
49	SOD2, mitochondrial	gi|31980762	24.6	High	3.58	–1.4	Yes (completely)
46	Esterase 1	gi|20070420	28.1	High	3.53	1.14	Yes (completely)
62	Myoglobin	gi|21359820	17.1	High	2.86	1.62	Yes (partially)
55	Myosin, light polypeptide 2, regulatory, cardiac, slow	gi|153791853	18.9	High	2.72	–4.76	Yes (completely)
12a	α_1 antitrypsin 1–3	gi|205371731	45.8	High	2.69	1.06	Yes (completely)
40	Myosin, light polypeptide 3	gi|33563264	22.4	High	2.66	1	Yes (completely)
69	mCG18900	gi|148705042	15.6	High	2.48	–1.11	Yes (completely)
18	ATP synthase, H+ transporting, mitochondrial F1 complex, β polypeptide	gi|23272966	56.6	High	2.43	1	Yes (completely)
61	Myoglobin	gi|21359820	17.1	High	2.35	–1.14	Yes (completely)
43	Prx3	gi|6680690	28.1	High	2.34	1.14	Yes (completely)
71	Ran/TC4 binding protein	gi|431422	23.6	*No*	2.23	–1.08	Yes (completely)
47	Esterase 1	gi|20070420	28.1	High	2.2	1.13	Yes (completely)
70	Iron/zinc purple acid phosphatase-like protein	gi|166979753	50.6	*No*	2.12	1	Yes (completely)
82	ATP synthase, H+ transporting, mitochondrial F0 complex, subunit d	gi|16741459	18.8	High	2.11	–1.15	Yes (completely)
21	Ubiquinol-cytochrome c reductase core protein 1	gi|46593021	52.8	High	2.01	–1.08	Yes (completely)
72	Centromere protein A, isoform CRA_b	gi|148705337	13.0	*No*	1.92	–1.07	Yes (completely)
30	Ubiquinol-cytochrome c reductase core protein 1	gi|3342500	35.6	High	1.91	–1.09	Yes (completely)
66	Cytochrome c oxidase, subunit IV, isoform 1	gi|6753498	19.5	High	1.9	–1.24	Yes (completely)
53	ATP synthase, H+ transporting, mitochondrial F0 complex, subunit d	gi|21313679	18.7	High	1.84	–1.17	Yes (completely)
45	mCG115348, isoform CRA_b	gi|148668894	25.4	High	1.83	1.6	No
22	α-cardiac actin	gi|387090	41.8	High	1.82	–1.03	Yes (completely)
25	Long-chain acyl-CoA dehydrogenase	gi|726095	48.1	High	1.81	–1.07	Yes (completely)
2a	Myosin binding protein C, cardiac	gi|161611787	140.5	High	1.76	1.52	No
12b	α_1 antitrypsin 1–3	gi|205371731	45.8	High	1.75	–1.05	Yes (completely)
33	Myozenin 2	gi|10946916	29.7	High	1.74	1.01	Yes (completely)
19	Sarcalumenin	gi|34328417	99.1	High	1.72	1	Yes (completely)
29	Isocitrate dehydrogenase 3 (NAD+) α	gi|148693875	34.6	High	1.68	–1.05	Yes (completely)
5	Muscle glycogen phosphorylase	gi|6755256	97.2	High	1.67	1.04	Yes (completely)
56	Unnamed protein product	gi|74198777	56.0	High	1.65	–1.13	Yes (completely)
20	Sarcalumenin, isoform CRA_a	gi|148664814	54.4	High	1.64	–1.07	Yes (completely)
36	mCG19938, isoform CRA_b	gi|148691000	39.7	High	1.6	–1.26	Yes (completely)
28	Aspartate aminotransferase	gi|871422	46.2	High	1.58	–1.04	Yes (completely)
51	mCG10592, isoform CRA_c	gi|148703873	16.5	High	1.58	–1.21	Yes (completely)
16	Pyruvate kinase, muscle	gi|31981562	57.8	High	1.54	–1.02	Yes (completely)

The data are listed according to the high-to-low fold change ratio of protein abundance between DOX and control hearts. The cut-off ratio was +1.5. The italic spot numbers (70, 71, and 72) in the first column indicate the low or no confidence on the protein spot identity as marked in the fifth column. MW: molecular weight; DOX: doxorubicin; FABP3: fatty acid binding protein 3; SOD: superoxide dismutase; Prx: peroxiredoxin.

Table 2 Cardiac proteins down-regulated by DOX: Effects of nitrate supplementation

2D-DIGE spot no.	Top -ranked protein name	Accession No.	Protein MW (kD)	Confidence of protein ID	DOX/control ratio	Nitrate + DOX/ control ratio	Reversed by nitrate
4	PYGB	gi|24418919	96.7	High	–6.24	–1.84	Yes (partially)
63	Unnamed protein product	gi|26350173	12.0	No	–3.42	2.07	Yes (completely)
42	mCG9061, isoform CRA_c	gi|148706375	28.4	High	–3.2	–2.2	Yes (partially)
15	Aldehyde dehydrogenase 4 family, member A1	gi|225543103	61.8	High	–3.11	–3.67	No
59	Peroxisomal membrane protein 20 (Prx5)	gi|6746357	17.0	High	–2.73	2.07	Yes (completely)
48	es1 protein	gi|20070420	28.1	High	–2.64	–3.27	No
68	ATP synthase, H+ transporting, mitochondrial F1 complex, δ subunit, isoform CRA_a	gi|148699643	14.3	High	–2.34	–2.75	No
39	Tyrosine 3-monooxygenase/ tryptophan	gi|148676868	29.1	High	–2.3	–1.43	Yes (completely)
13b	α1-antitrypsin 1–3	gi|205371731	45.8	High	–2.25	–1.17	Yes (completely)
23	Succinate-coenzyme A ligase, GDP-forming, β subunit	gi|165972309	46.8	High	–2.06	–1.29	Yes (completely)
52	MYL2	gi|199985	18.9	High	–2.03	2.79	Yes (completely)
54	Ferritin heavy chain 1	gi|6753912	21.1	High	–1.94	1.25	Yes (completely)
11	α-fetoprotein	gi|191765	47.2	High	–1.93	–1.3	Yes (completely)
67	ATP synthase, H+ transporting, mitochondrial F1 complex, δ subunit, isoform CRA_a	gi|148699643	14.3	High	–1.87	–1.97	No
57	Nucleoside-diphosphate kinase 2	gi|6679078	17.4	High	–1.7	–1.72	No
74	β_2-globin	gi|4760594	15.7	High	–1.68	–3.82	No
1a	Myosin, heavy polypeptide 6, cardiac muscle, α	gi|83405899	223.4	High	–1.67	–1.2	Yes (completely)
1b	Myosin, heavy polypeptide 6, cardiac muscle, α	gi|83405899	223.4	High	–1.56	–1.14	Yes (completely)
35	Four and a half LIM domains 2	gi|18204139	32.0	High	–1.54	–1.57	No
14	Fibrinogen, α polypeptide isoform 2	gi|33563252	61.3	High	–1.51	–1.66	No
13a	α1-antitrypsin 1–3	gi|205371731	45.8	High	–1.51	–1.14	Yes (completely)

The data are listed according to the high-to-low fold change ratio of protein abundance between DOX and control hearts. The cut-off ratio was –1.5. The italic spot number (63) in the first column indicates the low or no confidence on the protein spot identity as marked in the fifth column. MW: molecular weight; DOX: doxorubicin; PYGB: brain glycogen phosphorylase; Prx: peroxiredoxin; MYL: myosin light chain.

mCG115348, isoform CRA_b; spot #58 – *nucleoside-diphosphate kinase 2*). Furthermore, among the 20 identified protein spots down-regulated by DOX, 9 of them were completely reversed by nitrate supplementation (47%), 2 were partially reversed, and 8 were not affected (42%), as shown in Table 2. Figure 4 shows DeCyder 3D images highlighting the substantial differences in protein abundance between three treatment groups in five representative protein spots. The DOX-induced changes in these proteins and the normalizing effects of nitrate supplementation are easily visualized.

Classification of DOX-modified protein expression based on biological function

To further understand the functional significance of DOX-modified proteins in the heart, we grouped positively identified proteins according to their known biological function**s** (Table 3) under the following seven categories. The first group included three mitochondria-localized antioxidant proteins, *i.e.* SOD2, Prx3 and Prx5. The second group comprised 12 cytoskeletal/contractile proteins, in which 8 proteins were up-regulated and 4 were down-regulated by DOX. The myoglobin, identified at four different spots (#61, #62, #64, #65) in the 2D-DIGE gels, was consistently up-regulated by DOX, but completely reversed by nitrate (Tables 2 and 3). The third group included seven proteins that are involved in fatty acid or glucose metabolism. DOX treatment caused an increase in five of these metabolic proteins and a decrease in the remaining two. Most notably, an 8-fold enhancement in FABP3 (spot #73) was observed after DOX administration (Tables 1 and 3; Fig. 3), which was completely normalized by nitrate. Conversely, there was a 6-fold down-regulation of PYGB (spot #4) caused by DOX and nitrate supplementation partially reversed this trend.

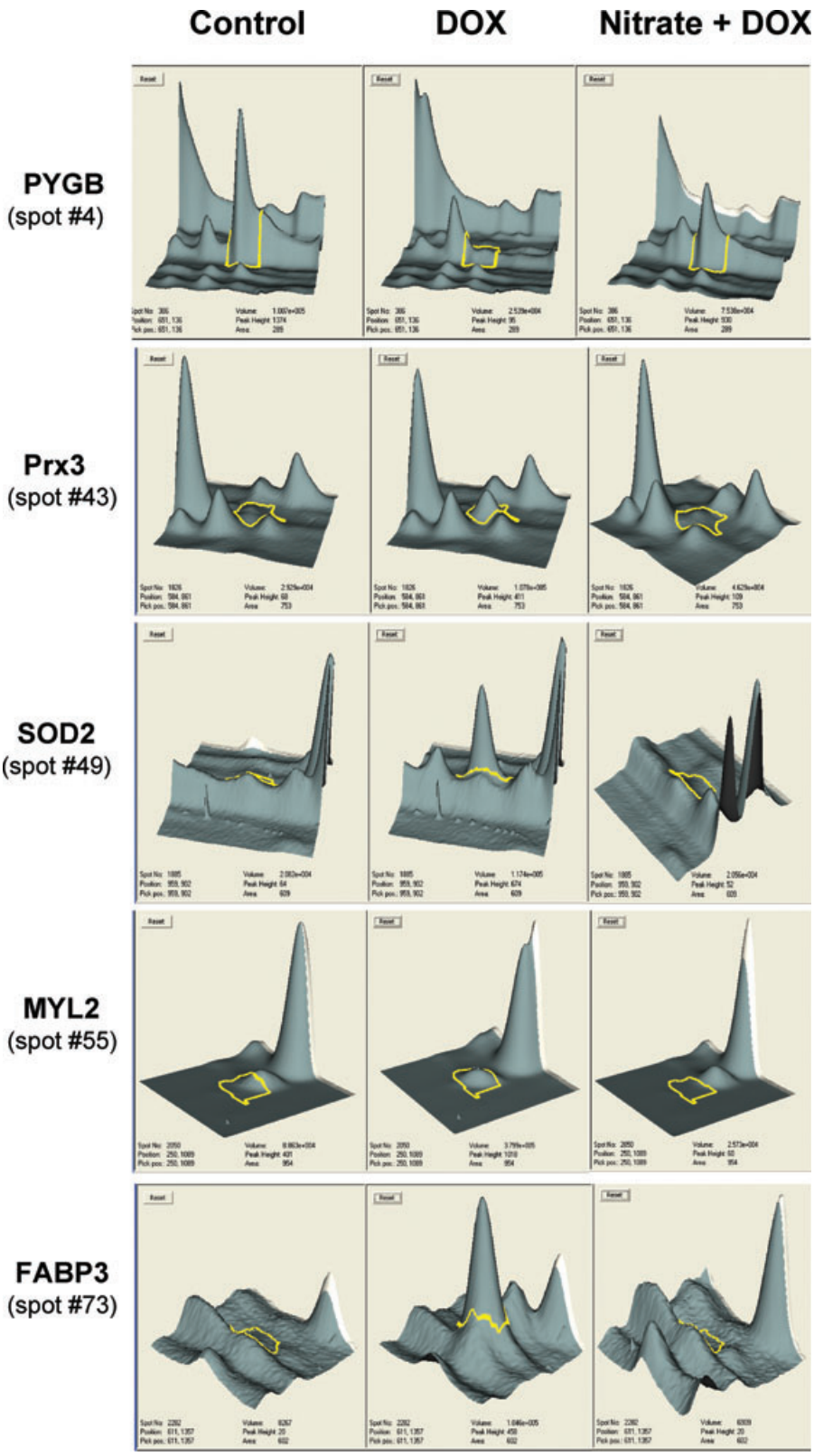

Fig. 4 Representative 3D DeCyder software integrated graphs showing differences in protein abundance. Five protein spots are selected from three treatment groups. Note that DOX-induced changes are normalized by nitrate supplementation. PYGB: brain glycogen phosphorylase; Prx3: peroxiredoxin 3; SOD2: mitochondrial superoxide dismutase 2; MYL2: myosin light chain 2; FABP3: fatty acid binding protein 3.

Table 3 DOX-modified cardiac proteins grouped based on biological function and the effects of nitrate supplementation on the modifications

Protein name	2D-DIGE spot	MW (kD)	DOX/control ratio	Nitrate effect
Antioxidant proteins				
SOD2, mitochondrial	49	24.6	3.58 ↑	Fully reversed
Prx3	43	28.1	2.34 ↑	Fully reversed
Peroxisomal membrane protein 20 (Prx5)	59	17.0	2.73 ↓	Fully reversed
Cytoskeletal/contractile proteins				
Myoglobin	61, 62, 64, 65	17.1	2.35–3.73 ↑	Fully reversed
Myosin, light polypeptide 2, regulatory, cardiac, slow	55	18.9	2.72 ↑	Fully reversed
Myosin, light polypeptide 3	40	22.4	2.66 ↑	Fully reversed
α-cardiac actin	22	41.8	1.82 ↑	Fully reversed
Myosin binding protein C, cardiac	2a	140.5	1.76 ↑	No effect
Myozenin 2	33	29.7	1.74 ↑	Fully reversed
Sarcalumenin	19	99.1	1.72 ↑	Fully reversed
Sarcalumenin, isoform CRA_a	20	54.4	1.64 ↑	Fully reversed
MYL2	52	18.9	2.03 ↓	Fully reversed
Ferritin heavy chain 1	54	21.1	1.94 ↓	Fully reversed
β_2-globin	74	15.7	1.68 ↓	No effect
Myosin, heavy polypeptide 6, cardiac muscle, α	1a, 1b	223.4	1.56–1.67 ↓	Fully reversed
Fatty acid/glucose metabolism proteins				
FABP3, muscle and heart	73	14.8	8.04 ↑	Fully reversed
Long-chain acyl-CoA dehydrogenase	25	48.1	1.81 ↑	Fully reversed
Isocitrate dehydrogenase 3 (NAD+) α	29	34.6	1.68 ↑	Fully reversed
Muscle glycogen phosphorylase	5	97.2	1.67 ↑	Fully reversed
Aspartate aminotransferase	28	46.2	1.58 ↑	Fully reversed
PYGB	4	96.7	6.24 ↓	Partially reversed
Succinate-Coenzyme A ligase, GDP-forming, β subunit	23	46.8	2.06 ↓	Fully reversed
Kinases				
Nucleoside-diphosphate kinase 2	58	17.4	4.18 ↑	No effect
Nucleoside-diphosphate kinase 2	57	17.4	1.70 ↓	No effect
Pyruvate kinase, muscle	16	57.8	1.54 ↑	Fully reversed
Mitochondrial respiratory chain				
ATP synthase, H+ transporting, mitochondrial F1 complex, β polypeptide	18	56.6	2.43 ↑	Fully reversed
ATP synthase, H+ transporting, mitochondrial F0 complex, subunit d	53, 82	18.8	1.84–2.11 ↑	Fully reversed
Ubiquinol-cytochrome c reductase core protein 1	21, 30	35.6, 52.8	1.91–2.01 ↑	Fully reversed
Cytochrome c oxidase, subunit IV, isoform 1	66	19.5	1.90 ↑	Fully reversed
ATP synthase, H+ transporting, mitochondrial F1 complex, δ subunit, isoform CRA_a	67, 68	14.3	1.87–2.34 ↓	No effect

Continued

Table 3 Continued

Protein name	2D-DIGE spot	MW (kD)	DOX/control ratio	Nitrate effect
Stress protein				
Crystallin, α_B	50	20.1	3.61 ↑	Fully reversed
Proteins with other function				
Esterase 1	46, 47	28.1	2.20–3.53 ↑	Fully reversed
α_1 antitrypsin 1–3	12a, 12b	45.8	1.75–2.69 ↑	Fully reversed
Aldehyde dehydrogenase 4 family, member A1	15	61.8	3.11 ↓	No effect
Esterase 1	48	28.1	2.64 ↓	No effect
α-fetoprotein	11	47.2	1.93 ↓	Fully reversed
Tyrosine 3-monooxygenase/ tryptophan	39	29.1	2.30 ↓	Fully reversed
Four and a half LIM domains 2	35	32.0	1.54 ↓	No effect
Fibrinogen, α polypeptide isoform 2	14	61.3	1.51 ↓	No effect

Note: The data are listed according to the high-to-low fold change ratio of protein abundance between DOX and control hearts. The cut-off ratio of change was $\pm$1.5. MW: molecular weight; DOX: doxorubicin; Prx: peroxiredoxin; SOD2: mitochondrial superoxide dismutase 2; MYL2: myosin light chain 2; FABP3: fatty acid binding protein 3; PYGB: brain glycogen phosphorylase.

DOX treatment caused alterations in two kinases (*i.e.* nucleoside-diphosphate kinase 2 and pyruvate kinase). The changes for nucleoside-diphosphate kinase 2 were identified in two separate spots (#57, #58) and neither of these was reversed by nitrate. However, DOX-induced mild increase in pyruvate kinase abundance was fully abolished by nitrate treatment. The fifth group included five proteins related to mitochondrial respiratory chain. There are three isoforms of ATP synthase (*i.e.* complex V), ubiquinol-cytochrome c reductase core protein 1 and cytochrome c oxidase (subunit IV). Majority of these mitochondrial proteins were increased by DOX treatment, which were reversed by nitrate supplementation. Interestingly, the δ subunit of F1 complex of ATP synthase was detected in two different spots (#67, #68) with opposing effects by DOX. Nevertheless, nitrate treatment had no effect on the DOX-induced changes.

In the sixth category, only one low molecular weight stress protein (α_B crystalline; spot #50) was increased ~3.6-fold by DOX, which was completely blunted by nitrate treatment.

Finally, there are eight positively identified proteins that have uncertain role in cardiac function. Among the six proteins down-regulated by DOX, four (*i.e.* aldehyde dehydrogenase 4 family, esterase 1, four and a half LIM domains 2, fibrinogen) were not affected by nitrate supplementation (Table 3).

Western blot analysis for verification of 2D-DIGE results

To confirm the 2D-DIGE results, DOX-induced six prominently modified proteins with known functional significance were probed by Western blots. These included antioxidant enzymes (SOD2, Prx3, Prx5), cytoskeletal/contractile protein (MYL2) and metabolic protein (FABP3, PYGB). To a larger extent, Western blot results confirmed most of the changes detected by 2D-DIGE for PYGB, SOD2, Prx3 and Prx5 (Figs 5 and 6). In contrast, two proteins (MYL2 and FABP3) showed opposite trend of the 2D-DIGE proteomic analysis (Fig. 5).

Effect of nitrate supplementation on mortality

As shown in Figure 7, 80% of the mice received DOX alone survived 5 days after the DOX injection. Nitrate supplemented mice in *Nitrate + DOX* group had a significantly higher survival rate (93%) as compared with *DOX* group ($P < 0.05$). There was no mortality in both *Control* and *Nitrate* alone groups during the entire 13-day experimental protocol.

Discussion

The cardiotoxicity of DOX remains an unsolved dilemma for both clinical and research communities. There is an ongoing call for a better therapeutic intervention to prevent and/or treat this devastating pathological condition of the heart. The present study was an extended endeavour to identify novel protein targets in protection against DOX-induced cardiomyopathy by inorganic nitrate supplementation [15, 16]. We utilized a globally non-biased proteomic approach with 2D-DIGE and MALDI TOF/TOF tandem mass spectrometry. The advantages of this method over conventional 2D gels in detecting global protein expression and post-translational

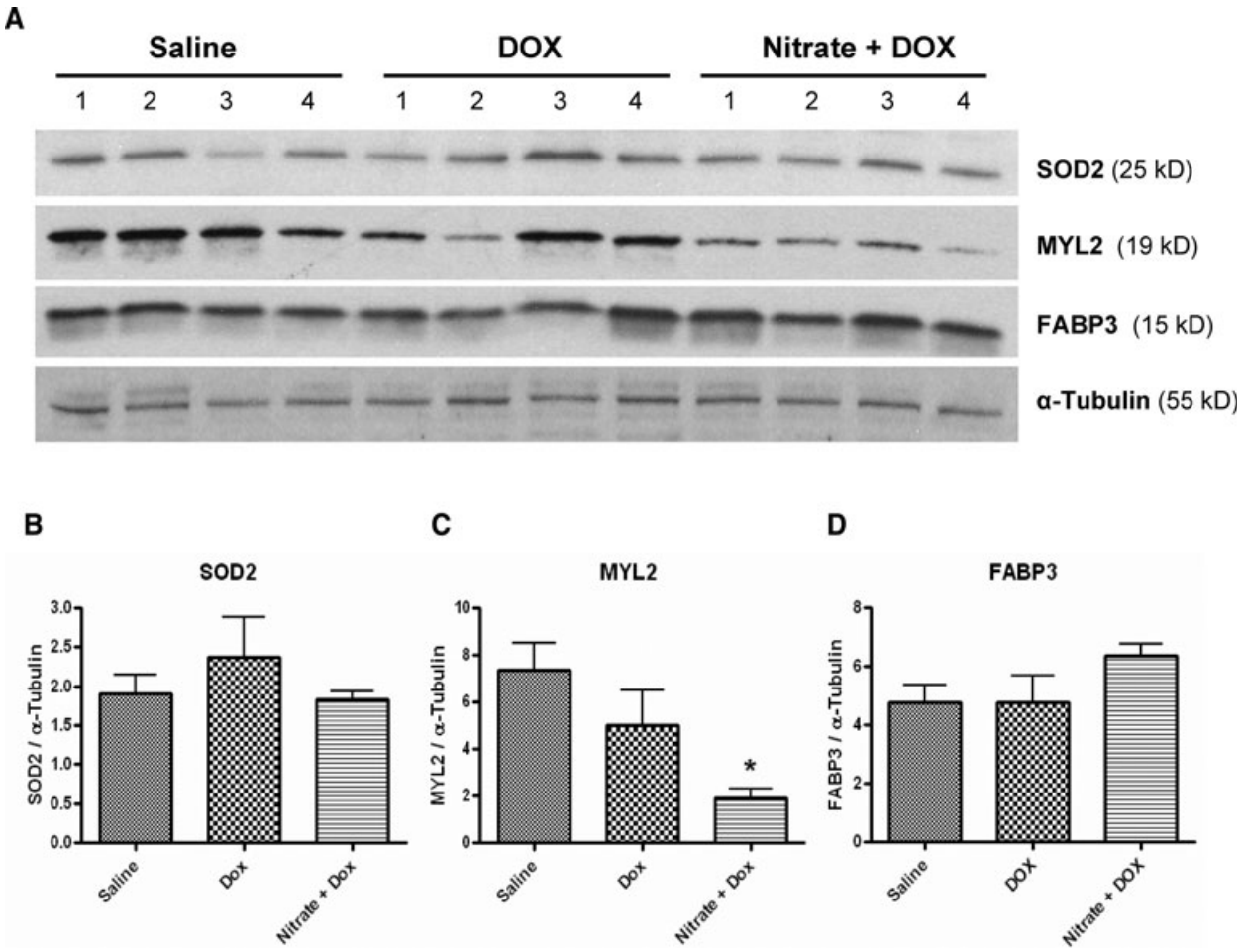

Fig. 5 (**A**) Western blots showing expression level of SOD2, MYL2 and FABP3. (**B**–**D**) Graphs for respective densitometric quantification of protein expression normalized against housekeeping protein α-Tubulin. Data are mean ± S.E.M. ($n = 4$ per group). * indicates $P < 0.05$ *versus Control*.

modifications have been increasingly appreciated in recent years [17, 18]. In particular, the conventional 2D gels methods are subject to inherent gel-to-gel variability and errors, which can be eliminated by multiplex, high-resolution 2D-DIGE technique. This technique uses both size- and charge-matched, spectrally resolvable fluorophores (CyDye) to simultaneously separate up to three samples on a single 2D gel. As a result, every protein spot on the gel has its own internal standard and direct comparisons between the samples can be made with high sensitivity without any gel-to-gel variability [17, 18].

One of the salient findings of the present study is the reversal in DOX-induced modification of three mitochondria-localized antioxidant enzymes (SOD2, Prx3, Prx5) by nitrate supplementation. Induction of cardiac SOD2 expression by DOX treatment has been reported by us [19] and others [20]. Because the protective role of SOD2 against DOX-induced cardiac injury has been well established by transgenic mice overexpressing SOD2 [21, 22], the up-regulation of SOD2 in the hearts from DOX-treated mice appears to be an adaptive response to DOX. However, the observed adaptive induction of cardiac SOD2 by DOX [19, 20] was not sufficient to prevent the DOX-induced cardiac ROS generation [23] and dysfunction [15]. The normalization of cardiac SOD2 expression by nitrate supplementation is likely due to the reduced level of oxidative stress following nitrate treatment that we recently reported [23]. Similarly, an increase of Prx3 was previously reported by Merten *et al.* [20]. Nitrate treatment completely restored Prx3 expression to its control level. On the other hand, Prx5 was the only thiol-based antioxidant that was up-regulated by the cardioprotective nitrate supplementation. Peroxiredoxin represents a new type of peroxidase distinct from catalase and glutathione peroxidase, in terms of abundance in expression, broad intracellular distribution, and high affinity for hydrogen peroxide [24, 25]. Among the total of six identified Prx isoforms, only Prx3 and Prx5 localize in mitochondria. Currently the role of Prx5 in protection against DOX-induced cardiotoxicity is unknown, although its importance in protecting cells against injuries caused

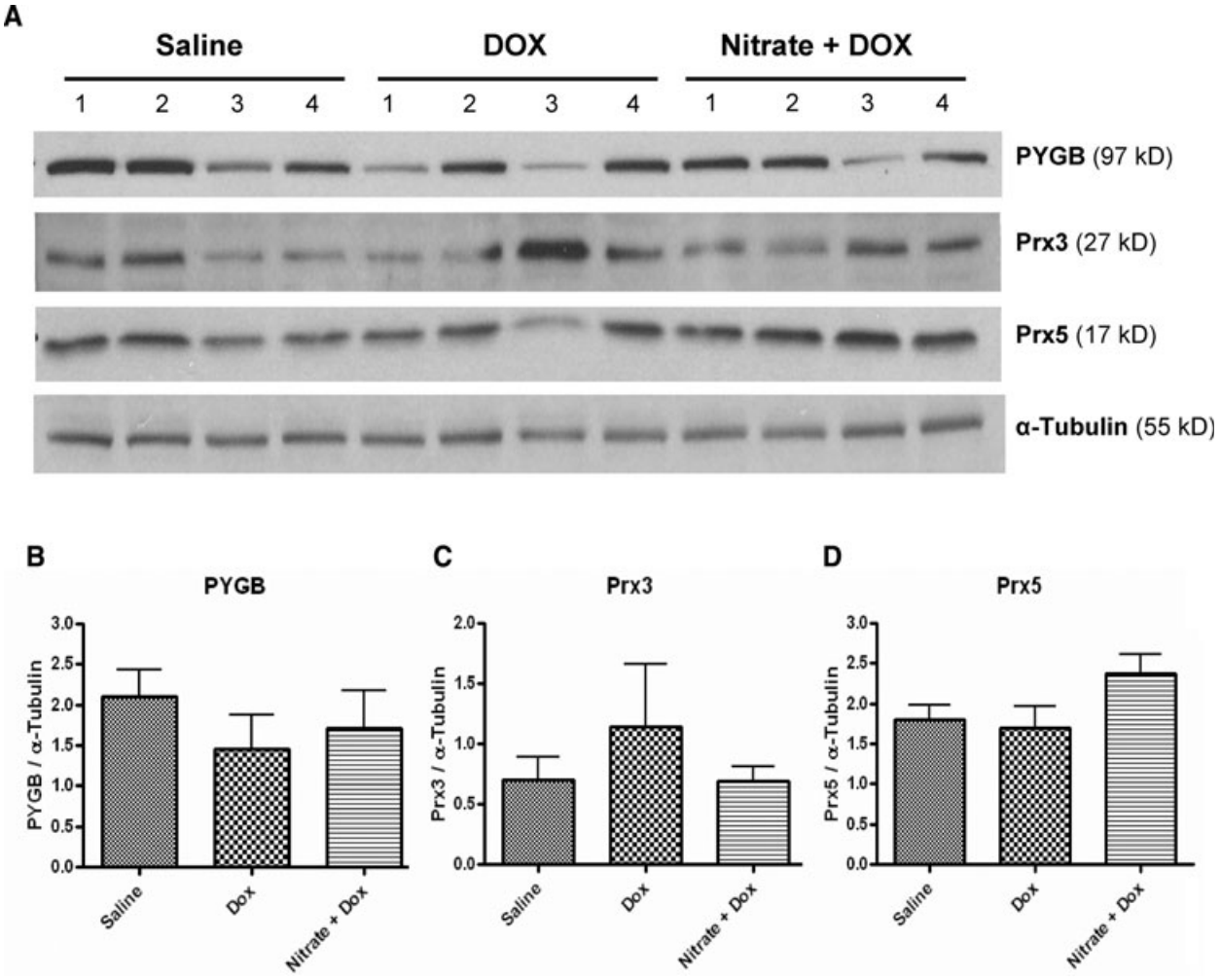

Fig. 6 (**A**) Western blots for PYGB, Prx3 and Prx5. (**B**–**D**) Graphs showing respective densitometric quantification of protein expression. Data are mean ± S.E.M. ($n = 4$ per group).

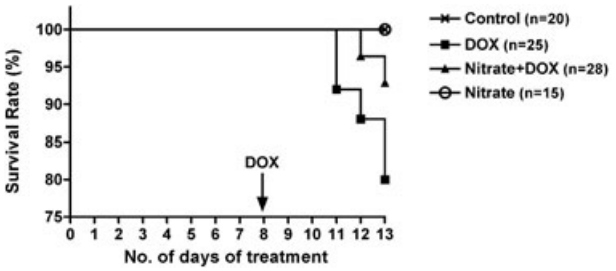

Fig. 7 Kaplan–Meier survival curves for the four treatment groups. The percentages of surviving mice are significantly different between the groups using the chi-square test ($n = 15$–28 per group, $P < 0.05$).

by reactive oxygen species (particularly hydrogen peroxide and peroxynitrite) has been suggested by several studies [26–29]. Further studies are needed to demonstrate a cause-and-effect relationship between induction of cardiac Prx5 and cardioprotection against DOX cardiotoxicity by nitrate supplementation.

It is noteworthy that Western blot results showed an opposite trend for the expression of MYL2 and FABP3 when compared with the 2D-DIGE results. We do not know the specific reason for these contrasting results. Nevertheless, it is possible that 2D-DIGE is a much more sensitive technique than the 1-D Western blots because it can identify changes occurring primarily in certain isoform(s) of a protein which may not be discernible by total protein expression that essentially detects all the isoforms with identical molecular weight.

Although a number of genomic studies have been reported to understand the mechanisms of DOX-induced cardiotoxicity [30, 31], only limited studies have used proteomic approaches which were specifically targeted toward comparing the protein

abundance between the DOX treatment with or without the cardioprotective intervention [20, 32–36], including transgenic overexpression of metallothionein [20], heat shock preconditioning [35] and co-treatment with docetaxel [33]. To our best knowledge, this is the first study using 2D-DIGE to determine alterations in cardiac proteins caused by DOX. Our results are particularly significant in terms of providing novel information on the reversal of DOX-induced modification of three mitochondrial antioxidant enzymes (SOD2, Prx3, Prx5) by nitrate supplementation, particularly the selective up-regulation of Prx5, which may play an important role in attenuating oxidative stress in the heart following nitrate supplementation [23].

Inorganic nitrate is a water soluble, very inexpensive chemical that appears ideal for long-term oral administration in preventing DOX-induced cardiomyopathy during its prolonged pathological process. On the other hand, there have been concerns on the potential toxic effects of high nitrate intake, particularly infant methemoglobinemia related to the high nitrate levels in drinking water and foods in certain areas such as Transylvania region of Romania [37] and the highly controversial issue of nitrate-induced carcinogenesis [38]. We cautiously believe that these potential side effects of nitrate are not present in the case of nitrate-induced protection against DOX cardiotoxicity. This is because methemoglobinemia rarely occurs in children or adults due to the physiological induction of methemoglobin reductase during the post-weaning developmental period [38]. Also, there should be no concern on the questionable carcinogenesis during the course of nitrate supplementation, because the targeted cancer patients would have already received anticancer therapy with DOX. Moreover, in the present study, the nitrate-supplemented mice had significantly higher survival rate (93%) than the controls (80%) 5 days after DOX treatment ($P < 0.05$), whereas the 13-day course of high nitrate intake alone did not cause any mortality or other apparent adverse effects in the mice.

The current upper limit of WHO acceptable intake (ADI) for nitrate is 222 mg per day for an adult with 60 kg body weight (*i.e.* 3.4 mg/kg) [39]. The oral nitrate dose used in the present study is about 180 mg/kg/day, which gives 14.6 mg/kg/day of human equivalent dose according to the FDA published conversion formula (*i.e.* mouse dose divided by 12.3). Therefore the nitrate dose is less than 400% of the WHO-ADI, which is within the physiological limits, considering particularly that just a cup of raw spinach contains 926 mg of nitrate [39]. Oral nitrate supplementation can be easily obtained from foods containing high levels of nitrate, *e.g.* leafy green vegetables [39] as well as from nitrate-enriched capsules and beverages that are already commercially available and safely used in human beings [40, 41]. Nitrate intake has been shown to exert a number of beneficial effects to attenuate myocardial ischemia-reperfusion injury [11, 12], hypertension [13, 14] and platelet aggregation [38]. In addition, nitrate supplementation has been shown to alleviate other degenerative chronic diseases such as type-2 diabetes [42], decreasing whole body oxygen cost during exercise and improving maximal performance [40, 41]. Taken together, it is conceivable that oral nitrate supplementation may have greater potential for clinical application in reducing cardiotoxicity, bodily suffering and financial burden of the thousands of cancer patients receiving DOX.

Acknowledgements

This study was supported in part by research grants from the National Institutes of Health (HL51045, HL79424, HL93685 to Dr. R.C.K.) and from the American Heart Association (National Scientist Development Grant #0530157N to Dr. L.X.). We thank Dr. John Liao of Applied Biomics, Inc. for his excellent technical support in proteomic analysis.

Conflict of interest

The authors confirm that there are no conflicts of interest.

References

1. **Bristow MR, Mason JW, Billingham ME, *et al.*** Doxorubicin cardiomyopathy: evaluation by phonocardiography, endomyocardial biopsy, and cardiac catheterization. *Ann Intern Med.* 1978; 88: 168–75.
2. **Steinherz LJ, Steinherz PG, Tan C.** Cardiac failure and dysrhythmias 6–19 years after anthracycline therapy: a series of 15 patients. *Med Pediatr Oncol.* 1995; 24: 352–61.
3. **Singal PK, Iliskovic N.** Doxorubicin-induced cardiomyopathy. *N Engl J Med.* 1998; 339: 900–5.
4. **Thompson KL, Rosenzweig BA, Zhang J, *et al.*** Early alterations in heart gene expression profiles associated with doxorubicin cardiotoxicity in rats. *Cancer Chemother Pharmacol.* 2010; 66: 303–14.
5. **Bolli R.** Cardioprotective function of inducible nitric oxide synthase and role of nitric oxide in myocardial ischemia and preconditioning: an overview of a decade of research. *J Mol Cell Cardiol.* 2001; 33: 1897–918.
6. **Ferdinandy P, Appelbaum Y, Csonka C, *et al.*** Role of nitric oxide and TPEN, a potent metal chelator, in ischaemic and reperfused rat isolated hearts. *Clin Exp Pharmacol Physiol.* 1998; 25: 496–502.
7. **Varga E, Bodi A, Ferdinandy P, *et al.*** The protective effect of EGb 761 in isolated ischemic/reperfused rat hearts: a link between cardiac function and nitric oxide production. *J Cardiovasc Pharmacol.* 1999; 34: 711–7.
8. **Xi L, Jarrett NC, Hess ML, *et al.*** Essential role of inducible nitric oxide synthase in monophosphoryl lipid A-induced late cardioprotection: evidence from pharmacological inhibition and gene knockout mice. *Circulation.* 1999; 99: 2157–63.

9. **Webb A, Bond R, McLean P, *et al.*** Reduction of nitrite to nitric oxide during ischemia protects against myocardial ischemia-reperfusion damage. *Proc Natl Acad Sci USA.* 2004; 101: 13683–8.
10. **Cosby K, Partovi KS, Crawford JH, *et al.*** Nitrite reduction to nitric oxide by deoxyhemoglobin vasodilates the human circulation. *Nat Med.* 2003; 9: 1498–505.
11. **Bryan NS, Calvert JW, Elrod JW, *et al.*** Dietary nitrite supplementation protects against myocardial ischemia-reperfusion injury. *Proc Natl Acad Sci USA.* 2007; 104: 19144–9.
12. **Duranski MR, Greer JJ, Dejam A, *et al.*** Cytoprotective effects of nitrite during *in vivo* ischemia-reperfusion of the heart and liver. *J Clin Invest.* 2005; 115: 1232–40.
13. **Tsuchiya K, Kanematsu Y, Yoshizumi M, *et al.*** Nitrite is an alternative source of NO *in vivo*. *Am J Physiol Heart Circ Physiol.* 2005; 288: H2163–70.
14. **Kapil V, Milsom AB, Okorie M, *et al.*** Inorganic nitrate supplementation lowers blood pressure in humans: role for nitrite-derived NO. *Hypertension.* 2010; 56: 274–81.
15. **Zhu SG, Das A, Xi L, *et al.*** Dietary supplementation of nitrate protects against doxorubicin-induced ventricular dysfunction and cardiomyocyte cell death in mice. *Circulation.* 2008; 118: S945 (abstract).
16. **Chen Q, Zhu SG, Lesnefsky EJ, *et al.*** Chronic dietary supplementation of nitrate prevents doxorubicin-induced cardiac mitochondrial damage. *Circulation.* 2009; 120: S867 (abstract).
17. **Marouga R, David S, Hawkins E.** The development of the DIGE system: 2D fluorescence difference gel analysis technology. *Anal Bioanal Chem.* 2005; 382: 669–78.
18. **Moore JC, Fu J, Chan YC, *et al.*** Distinct cardiogenic preferences of two human embryonic stem cell (hESC) lines are imprinted in their proteomes in the pluripotent state. *Biochem Biophys Res Commun.* 2008; 372: 553–8.
19. **Koka S, Das A, Zhu SG, *et al.*** Long-acting phosphodiesterase-5 inhibitor tadalafil attenuates doxorubicin-induced cardiomyopathy without interfering with chemotherapeutic effect. *J Pharmacol Exp Ther.* 2010; 334: 1023–30.
20. **Merten KE, Feng W, Zhang L, *et al.*** Modulation of cytochrome C oxidase-va is possibly involved in metallothionein protection from doxorubicin cardiotoxicity. *J Pharmacol Exp Ther.* 2005; 315: 1314–9.
21. **Yen HC, Oberley TD, Vichitbandha S, *et al.*** The protective role of manganese superoxide dismutase against adriamycin-induced acute cardiac toxicity in transgenic mice. *J Clin Invest.* 1996; 98: 1253–60.
22. **Yen HC, Oberley TD, Gairola CG, *et al.*** Manganese superoxide dismutase protects mitochondrial complex I against adriamycin-induced cardiomyopathy in transgenic mice. *Arch Biochem Biophys.* 1999; 362: 59–66.
23. **Chen Q, Zhu S-G, Lesnefsky EJ, *et al.*** Chronic dietary supplementation of nitrate decreases doxorubicin-induced oxidative stress in cardiac mitochondria and tissues. *Circulation.* 2010; 122, A15894 (abstract).
24. **Rhee SG, Chae HZ, Kim K.** Peroxiredoxins: a historical overview and speculative preview of novel mechanisms and emerging concepts in cell signaling. *Free Radic Biol Med.* 2005; 38: 1543–52.
25. **Kang SW, Rhee SG, Chang TS, *et al.*** 2-Cys peroxiredoxin function in intracellular signal transduction: therapeutic implications. *Trends Mol Med.* 2005; 11: 571–8.
26. **Plaisant F, Clippe A, Vander SD, *et al.*** Recombinant peroxiredoxin 5 protects against excitotoxic brain lesions in newborn mice. *Free Radic Biol Med.* 2003; 34: 862–72.
27. **Banmeyer I, Marchand C, Clippe A, *et al.*** Human mitochondrial peroxiredoxin 5 protects from mitochondrial DNA damages induced by hydrogen peroxide. *FEBS Lett.* 2005; 579: 2327–33.
28. **Trujillo M, Clippe A, Manta B, *et al.*** Pre-steady state kinetic characterization of human peroxiredoxin 5: taking advantage of Trp84 fluorescence increase upon oxidation. *Arch Biochem Biophys.* 2007; 467: 95–106.
29. **Abbas K, Breton J, Picot CR, *et al.*** Signaling events leading to peroxiredoxin 5 up-regulation in immunostimulated macrophages. *Free Radic Biol Med.* 2009; 47: 794–802.
30. **Ito H, Miller SC, Billingham ME, *et al.*** Doxorubicin selectively inhibits muscle gene expression in cardiac muscle cells *in vivo* and *in vitro*. *Proc Natl Acad Sci USA.* 1990; 87: 4275–9.
31. **Yi X, Bekeredjian R, DeFilippis NJ, *et al.*** Transcriptional analysis of doxorubicin-induced cardiotoxicity. *Am J Physiol Heart Circ Physiol.* 2006; 290: H1098–102.
32. **Chen Y, Daosukho C, Opii WO, *et al.*** Redox proteomic identification of oxidized cardiac proteins in adriamycin-treated mice. *Free Radic Biol Med.* 2006; 41: 1470–7.
33. **Ohyama K, Tomonari M, Ichibangase T, *et al.*** A toxicoproteomic study on cardioprotective effects of pre-administration of docetaxel in a mouse model of adriamycin-induced cardiotoxicity. *Biochem Pharmacol.* 2010; 80: 540–7.
34. **Vedam K, Nishijima Y, Druhan LJ, *et al.*** Role of heat shock factor-1 activation in the doxorubicin-induced heart failure in mice. *Am J Physiol Heart Circ Physiol.* 2010; 298: H1832–41.
35. **Venkatakrishnan CD, Tewari AK, Moldovan L, *et al.*** Heat shock protects cardiac cells from doxorubicin-induced toxicity by activating p38 MAPK and phosphorylation of small heat shock protein 27. *Am J Physiol Heart Circ Physiol.* 2006; 291: H2680–91.
36. **Xie L, Terrand J, Xu B, *et al.*** Cystatin C increases in cardiac injury: a role in extracellular matrix protein modulation. *Cardiovasc Res.* 2010; 87: 628–35.
37. **Ayebo A, Kross BC, Vlad M, *et al.*** Infant Methemoglobinemia in the Transylvania Region of Romania. *Int J Occup Environ Health.* 1997; 3: 20–9.
38. **McKnight GM, Duncan CW, Leifert C, *et al.*** Dietary nitrate in man: friend or foe? *Br J Nutr.* 1999; 81: 349–58.
39. **Hord NG, Tang Y, Bryan NS.** Food sources of nitrates and nitrites: the physiologic context for potential health benefits. *Am J Clin Nutr.* 2009; 90: 1–10.
40. **Bailey SJ, Winyard P, Vanhatalo A, *et al.*** Dietary nitrate supplementation reduces the O_2 cost of low-intensity exercise and enhances tolerance to high-intensity exercise in humans. *J Appl Physiol.* 2009; 107: 1144–55.
41. **Larsen FJ, Weitzberg E, Lundberg JO, *et al.*** Dietary nitrate reduces maximal oxygen consumption while maintaining work performance in maximal exercise. *Free Radic Biol Med.* 2010; 48: 342–7.
42. **Carlstrom M, Larsen FJ, Nystrom T, *et al.*** Dietary inorganic nitrate reverses features of metabolic syndrome in endothelial nitric oxide synthase-deficient mice. *Proc Natl Acad Sci USA.* 2010; 107: 17716–20.